Report worksheet 3

Joaquín Rapela

February 17, 2023

Exercise 1: LFPs

Figure 1 shows the LFP for a few selected channels.

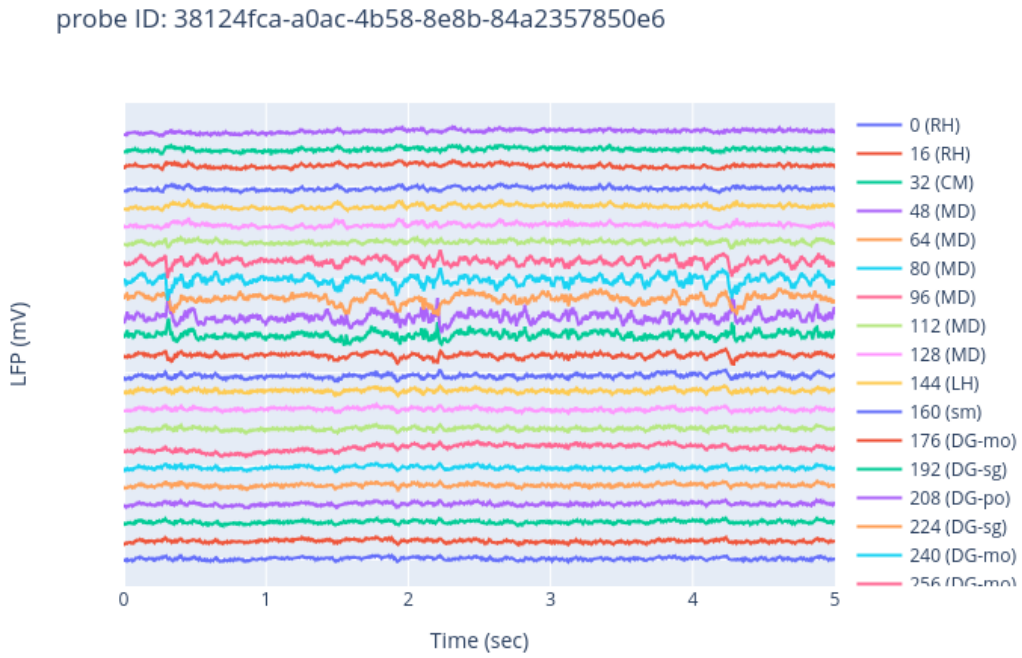

Figure 1: LFP of selected channels. The script to generate this figure appears here and the parameters used with this script appear here. Click on the figure to view its interactive version.

Exercise 2: power spectrum

Figure 2 shows the power spectrum for all channels.

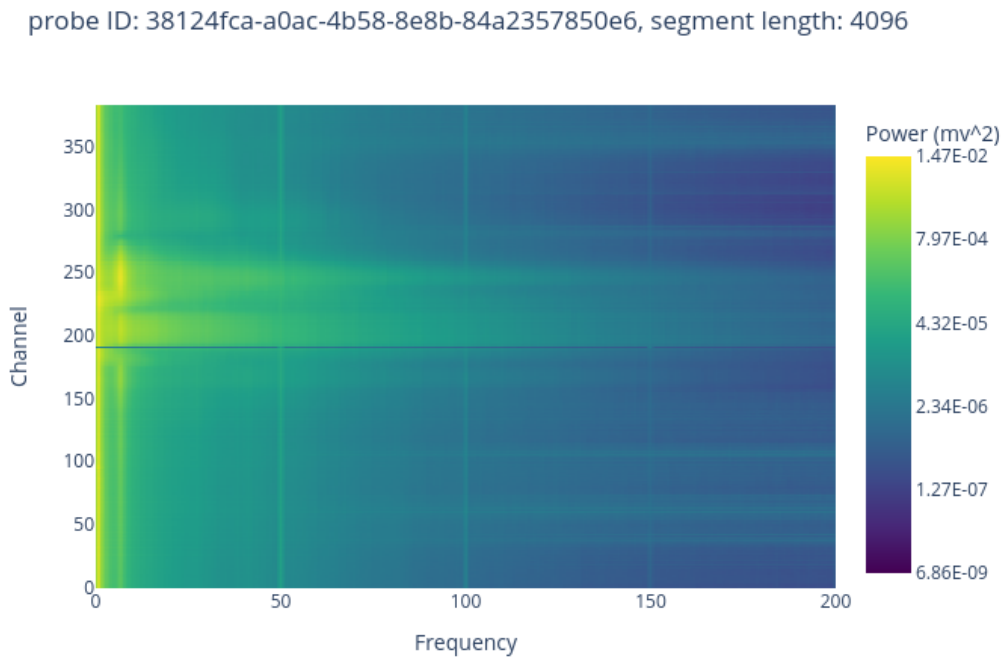

Figure 2: Power spectrum of all channels. To overcome memory problems related from retrieving large LFPs, we estimated this power spectrum using only 600 seconds of LFPs. We used the Welch method (as implemented in the Python function `scipy.signal.pwelch`) with a window of length 4096 samples, or 1.64 seconds, giving a frequency resolution of $1/1.64 = 0.61$ Hz (`scipy.signal.pwelch` parameter `nperseg`=4096). We generated this figure using this script, with its default parameters. Click on the figure to view its interactive version.

The formula for the frequency resolution (in Hz) is $\texttt{freq\_res\_HZ} = \frac{1}{\texttt{data\_len\_sec}}$, where `data_len_sec` is the length of the data (in seconds) used to calculate the Fourier transform. Because the Welch method to estimate the power spectrum computes the Fourier transform using data of the length of its window, to obtain a frequency resolution less than 1 Hz, we need a window of length greater than one second, or greater than $sr.fs = 2.500$ samples. We used 4,096 samples to estimate the power spectrums in Figure 2.

We see large power around 7 Hz (theta band) in electrodes in the dentate gyrus. Oscillations in the theta range in the dentate gyrus have been previously reported (e.g., Rangel et al., 2015).

We observe stripes of high power at multiples of 50 Hz, that correspond to contamination of the recordings by the AC power line, which in the UK operates at 50 Hz. Why do we see high power stripes at multiples of 50 Hz (i.e., 100 Hz or 150 Hz)? This is because, as proved in Lemma 1 in the appendix, the Fourier representation of a periodic continuous signal (like the AC current) is a scaled set of delta functions at multiples of the frequency of the periodic signal.

Exercise 3: spectrogram

Figure 3 shows the spectrogram for channel 250, calculated with LFP data of length 1,000 seconds, starting at time 4,500 seconds.‘

To overcome the memory problem related to loading large LFP data (i.e., multiple channels and long duration), we estimated several spectrograms, with different start times, on windows of length 1.000 seconds. We only found evidence of power line contamination in the spectrogram calculated with LFP data starting at time of 4,500 seconds.

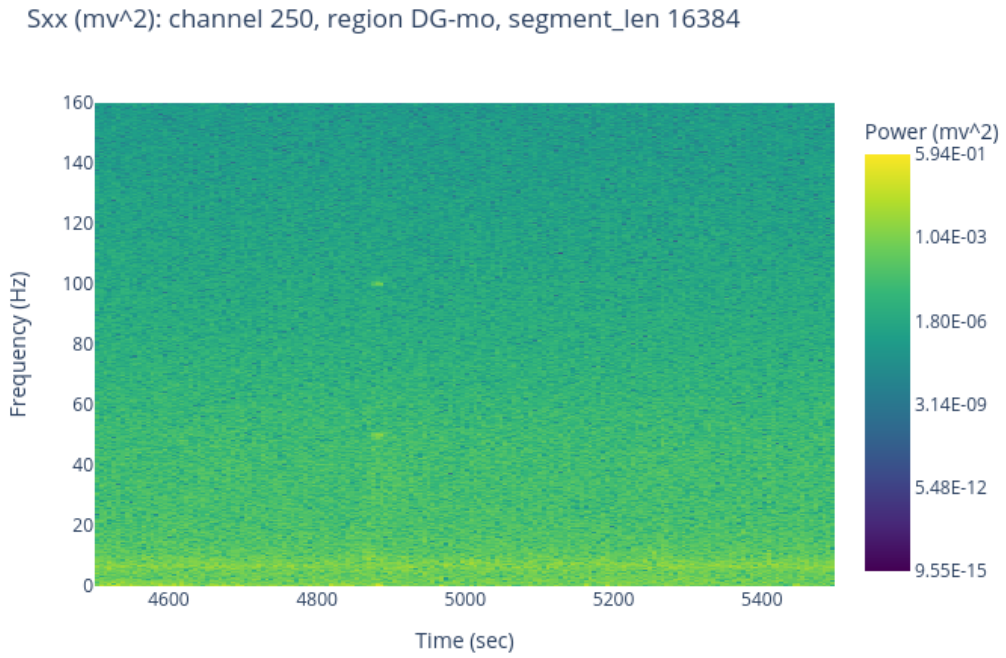

Figure 3: Spectrogram of channel 250 calculated from LFP data between 4,500 and 5,500 seconds. Estimation was done using the method `scipy.signal.spectrogram` with a window length of `nperseg`=16,384 samples=6.55 seconds. The script to generate this figure appears here, and the parameters used with this script appear here Click on the figure to view its interactive version.

Exercise 4: comodugram

Figure 4 shows the comodugram for channel 250.

To overcome the memory problem related to loading large LFP data (i.e., multiple channels and long duration), we used a computer with very large RAM memory.

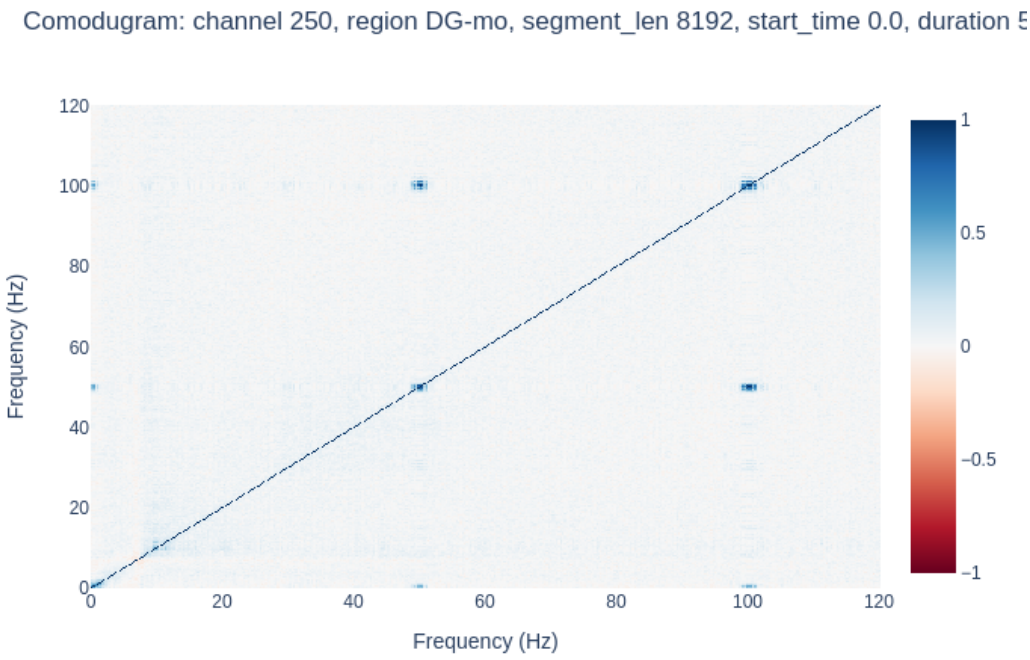

Figure 4: Comodugram for channel 250. Estimation was done using 5,500 seconds of LFP data, starting at time zero. We first computed the spectrogram using the method `scipy.signal.spectrogram` with a window length of `nperseg`=8,192 samples=3.28 seconds, and then calculated the Pearson correlation coefficient between power at different frequencies using function `np.corrcoef`. We generated this figure with this script using its default parameters. Click on the figure to view its interactive version.

We see that power at 50 Hz and 100 Hz are highly correlated due to the harmonics generated by the power line. The blue spots around 8 Hz show that the theta rhythm in the dentate gyrus appears in a broad set of frequencies around 8 Hz, and that power at these frequencies is correlated.

Exercise 5: coherence

Figure 5 shows the coherence between channel 250 and the other channels.

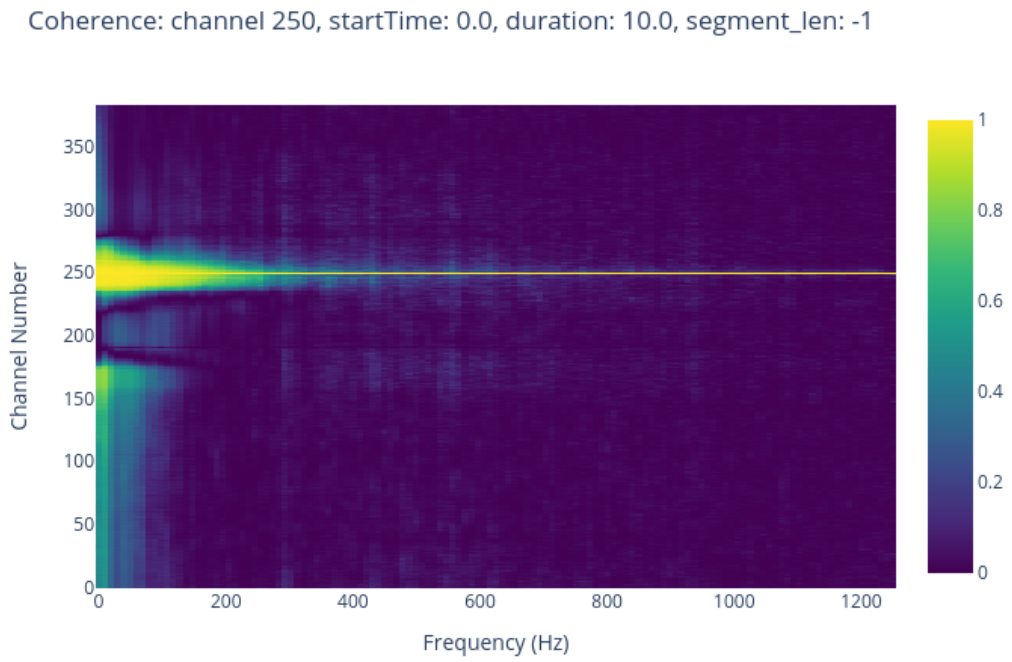

Figure 5: Coherence between channel 250 and the other channels. Estimation was done using 10 seconds of LFP data, starting at time 0, with the method `scipy.signal.coherence`. We generated this figure with this script, using its default parameters. Click on the figure to view its interactive version.

The strip at channel 250 indicates a linear phase relation between the LFP of this channel and itself at all frequencies. More interestingly, at frequencies below 150 Hz we observe large coherence (i.e., linear phase relations) limited to channels in the dentate gyrus molecular layer.

Exercise 6: cross-spectrum phase

Figure 6 shows the cross-spectrum phase between channel 250 and the other channels.

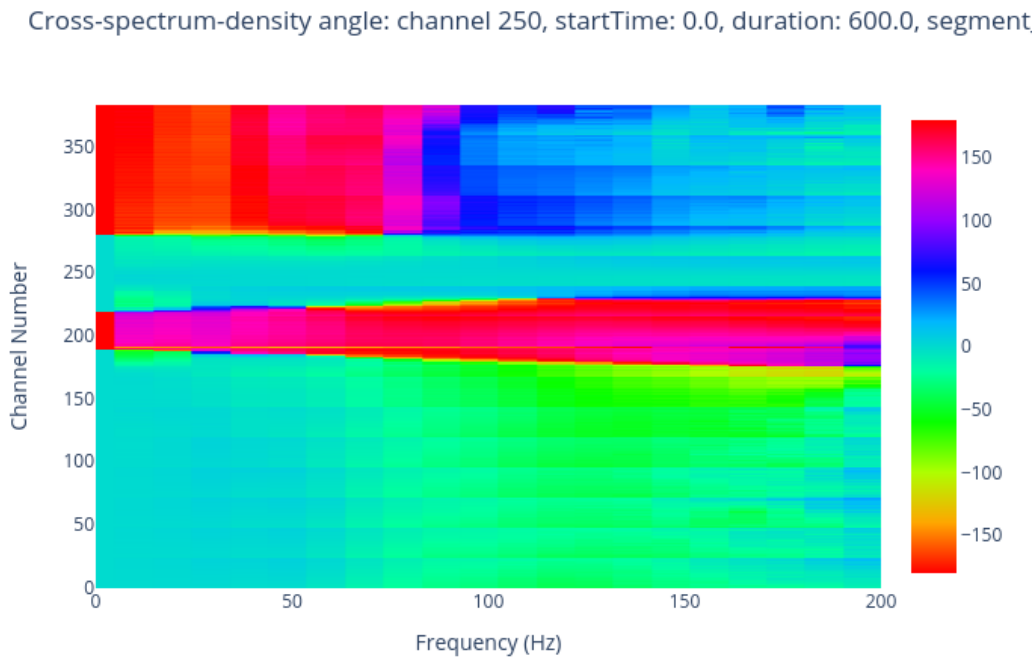

Figure 6: Cross-spectrum phase between channel 250 and the other channels. Estimation was done using the method `scipy.signal.csd` in a time window of 600 seconds starting at time zero. We generated this figure with this script, using its default parameters. Click on the figure to view its interactive version.

Figure 6 shows that channel 250 is approximately 180 degrees out of phase with channels 200 and 300, and approximately in phase with channel 170.

Figure 2 shows that the largest power at channel 200 (0.003 mV^2) is comparable to that at channel 250 (0.008 mV^2), but an order of magnitude larger than the maximum power at channel 300. (0.0005 mV^2). Thus, the phase difference with channel 250 should be more apparent for channel 200 than for channel 300, as illustrated in Figure 7. Also the largest power at channel 170 (0.001 mV^2) is intermediate with that of channels 200 and 300. Thus, the phase relation of channel 250 with channel 170 should be less apparent than that with channel 200, but more apparent than that with channel 300, as also shown in Figure 7.

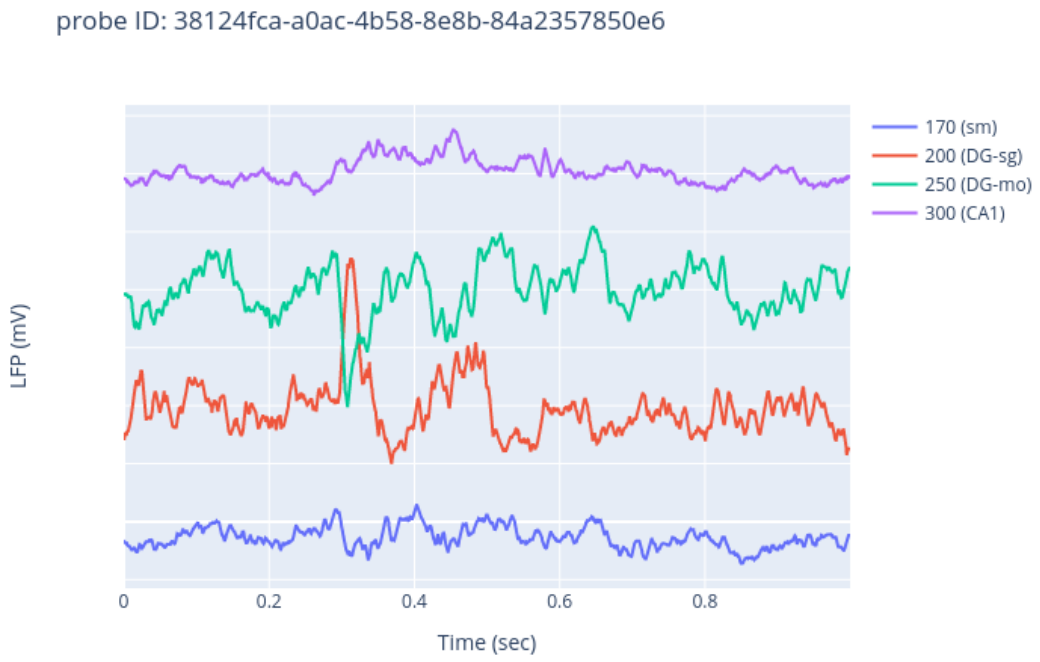

Figure 7: LFP of channels 170, 200, 250 and 300. These LFPs agree with Figure 6 in that the LFP at channel 250 has opposite phase than that at channel 200 and 300, but similar phase than the LFP at channel 170. The script used to generate this figure appears here and the parameters used with this script appear here. Click on the figure to view its interactive version.

Appendix A Fourier transform of a continuous periodic signal

We prove in Lemma 1 that the Fourier transform of a continuous periodic signal is a sum of scaled delta functions at multiples of the frequency of this signal.

Definition 1 (continuous signal)**.** *A continuous signal $x(t)$ is periodic if and only if there exists a period $T > 0$ such that*

$$x(t) = x(t+T), \forall t \in \Re \tag{1}$$

Lemma 1 (Fourier transform of a periodic signal)**.** *If $x(t)$ is periodic, with period T, then*

$$\mathcal{FT}\{x(t)\}(j\Omega) = 2\pi \sum_{k=-\infty}^{\infty} X^S[k]\ \delta\left(\Omega - \frac{2\pi k}{T}\right) \tag{2}$$

with $X^S[k]$ the Fourier series coefficient at frequency k (Eq. 4).

Proof. Because $x(t)$ is a periodic signal, it admits a Fourier series representation (Porat, 1997, Section 2.3)

$$x(t) = \sum_{k=-\infty}^{\infty} X^S[k] \exp\left(\frac{j2\pi kt}{T}\right) \tag{3}$$

with

$$X^S[k] = \frac{1}{T}\int_{-T/2}^{T/2} x(t) \exp\left(-\frac{j2\pi kt}{T}\right) \tag{4}$$

By the linearity of the Fourier transform (Porat, 1997, Eq. 2.4), from Eq. 3, we have

$$\mathcal{FT}\{x(t)\}(j\Omega) = \sum_{k=-\infty}^{\infty} X^S[k]\ \mathcal{FT}\left\{\exp\left(\frac{j2\pi kt}{T}\right)\right\}(j\Omega) \tag{5}$$

We next compute the Fourier transform of the exponential in the right hand side of Eq. 5

$$\mathcal{FT}\left\{\exp\left(\frac{j2\pi kt}{T}\right)\right\}(j\Omega) = \mathcal{FT}\left\{1\ \exp\left(\frac{j2\pi kt}{T}\right)\right\}(j\Omega) \tag{6}$$

$$= \mathcal{FT}\{1\}\left(j\left(\Omega - \frac{2\pi k}{T}\right)\right) \tag{7}$$

$$= 2\pi\ \delta\left(\Omega - \frac{2\pi k}{T}\right) \tag{8}$$

Notes:

1. Eq. 7 follows from Eq. 6 by the the frequency shift property of the Fourier transform[1].
2. Eq. 8 follows from Eq. 7 by the Fourier transform of the DC function (Lemma 2).

Replacing Eq. 8 into Eq. 5 yields Eq. 2.

□

Lemma 2 (Fourier transform of the DC function)**.**

$$\mathcal{FT}\{1\}(j\Omega) = 2\pi\ \delta(\Omega) \tag{9}$$

Proof. We start by computing the Fourier transform of the delta function.

$$\mathcal{FT}\{\delta(t)\}(j\Omega) = \int_{-\infty}^{\infty} \delta(t) \exp\left(-j\Omega t\right)\ dt = \exp\left(-j\Omega t\right)|_{t=0} = 1 \tag{10}$$

Then by the duality property of the Fourier transform (Lemma 3) we have

$$\mathcal{FT}\{1\}(j\Omega) = 2\pi\ \delta(-\Omega) = 2\pi\ \delta(\Omega) \tag{11}$$

Notes:

1. The last equality in Eq. 11 holds because the delta function is even.

□

Lemma 3 (Duality of the Fourier transform)**.** *Let $x(t)$ be a signal and $X(j\Omega)$ be its Fourier transform, then*

$$\mathcal{FT}\{X(jt)\}(j\Omega) = 2\pi\ x(-\Omega) \tag{12}$$

Proof. If $x(t)$ is a signal, with real or complex values, and $X(j\Omega)$ is its Fourier transform, then they are related by the following equations (Porat, 1997, Section 2.1)

$$X(j\Omega) = \mathcal{FT}\{x(t)\}(j\Omega) = \int_{-\infty}^{\infty} x(t) \exp\left(-j\Omega t\right) dt \tag{13}$$

$$x(t) = \mathcal{IFT}\{X(j\Omega)\}(t) = \frac{1}{2\pi} \int_{-\infty}^{\infty} X(j\Omega) \exp\left(j\Omega t\right) d\Omega \tag{14}$$

Then

[1] $y(t) = e^{j\Omega_0 t} x(t) \leftrightarrow Y(j\Omega) = X\left(j(\Omega - \Omega_0)\right)$, Porat (1997, Section 2.1)

$$\mathcal{FT}\left\{X(jt)\right\}(j\Omega) = \int_{-\infty}^{\infty} X(jt)\exp\left(-j\Omega t\right)dt \tag{15}$$

$$= 2\pi\left(\frac{1}{2\pi}\int_{-\infty}^{\infty} X(jt)\exp\left(jt(-\Omega)\right)dt\right) \tag{16}$$

$$= 2\pi\, x(-\Omega) \tag{17}$$

Notes:

1. in Eq. 15 we applied the Fourier transform (Eq. 13) to the complex signal $X(jt)$
2. in Eq. 17 we used the inverse Fourier transform (Eq. 14) with the change of variables Ω in Eq. 14 to t in Eq. 16 and t in Eq. 14 to $-\Omega$ in Eq. 16.

□

References

Porat, B. (1997). *A course in digital signal processing*. John Wiley & Sons, Inc.

Rangel, L. M., Chiba, A. A., and Quinn, L. K. (2015). Theta and beta oscillatory dynamics in the dentate gyrus reveal a shift in network processing state during cue encounters. *Frontiers in systems neuroscience*, page 96.